Mst1 regulates non-small cell lung cancer A549 cell apoptosis by inducing mitochondrial damage via ROCK1/F-actin pathways

WEIQIANG ZHANG, KEIQIANG LIU, YINGXIN PEI, JINGBO MA, JIANG TAN and JING ZHAO

Department of Thoracic Surgery, Army General Hospital of PLA, Beijing 100700, P.R. China

Abstract. Mammalian STE20-like kinase 1 (Mst1) is well recognized as a major tumor suppressor in cancer development, growth, metabolic reprogramming, metastasis, cell death and recurrence. However, the roles of Mst1 in non-small cell lung cancer (NSCLC) A549 cell phenotypic alterations remain to be elucidated. The present study aimed to explore the functional role and underlying mechanisms of Mst1 with regards to A549 cell proliferation, migration and apoptosis; this study focused on mitochondrial homeostasis and Rho-associated coiled-coil containing protein kinase 1 (ROCK1)/F-actin pathways. The results demonstrated that Mst1 was downregulated in A549 cells compared with in a normal pulmonary epithelial cell line. Subsequently, overexpression of Mst1 in A549 cells reduced cell viability and promoted cell apoptosis. Furthermore, overexpression of Mst1 suppressed A549 cell proliferation and migration. At the molecular level, the reintroduction of Mst1 in A549 cells led to activation of mitochondrial apoptosis, as evidenced by a reduction in mitochondrial potential, overproduction of ROS, cytochrome c release from the mitochondria into the nucleus, and upregulation of pro-apoptotic protein expression. In addition, Mst1 overexpression was closely associated with impaired mitochondrial respiratory function and suppressed cellular energy metabolism. Functional studies illustrated that Mst1 overexpression activated ROCK1/F-actin pathways, which highly regulate mitochondrial function. Inhibition of ROCK1/F-actin pathways in A549 cells sustained mitochondrial homeostasis, alleviated caspase-9-dependent mitochondrial apoptosis, enhanced cancer cell migration and increased cell proliferation. In conclusion, these data firmly established the regulatory role of Mst1 in NSCLC A549 cell survival via the modulation of ROCK1/F-actin pathways, which may provide opportunities for novel treatment modalities in clinical practice.

Correspondence to: Dr Jing Zhao, Department of Thoracic Surgery, Army General Hospital of PLA, 5 Nanmencang Street, Dongcheng, Beijing 100700, P.R. China
E-mail: congcong.01@163.com

Introduction

At present, non-small cell lung cancer (NSCLC) is one of the leading causes of cancer-associated mortality in elderly patients. Although the early treatment for NSCLC has improved in recent years, including platinum-based chemotherapy and radiotherapy, NSCLC remains an aggressive type of cancer, and the majority of patients have a poor prognosis, since NSCLC is typically detected at the late stages of the disease (1). Excessive cancer cell migration and survival are known to serve a crucial role in the development and progression of NSCLC (2). Accordingly, suppressing cancer cell migration and survival is vital for slowing or preventing NSCLC progression.

Mammalian STE20-like kinase 1 (Mst1) is an element of the Hippo pathway, which was initially identified as a major growth suppressor that interrupts stem cell growth, proliferation and apoptosis (3). Subsequent studies have illustrated that Mst1 is also involved in sustaining cardiomyocyte survival in diabetic cardiomyopathy (4,5), suppressing endometrial stromal cell migration in endometriosis (6) and promoting cancer cell apoptosis in colorectal carcinoma (7). These findings indicated that Mst1 functions as a tumor suppressor by modulating cancer cell apoptosis, migration and proliferation. However, the role of Mst1 in NSCLC A549 cells remains to be elucidated.

Mitochondria are vital for cancer development (8). Mitochondria are at the center of energy production, and damage to mitochondria reduces cancer metabolism and therefore limits cancer growth (9). In addition, mitochondria are messengers of cellular apoptotic signals; poorly structured mitochondria release the pro-apoptotic factor cytochrome c (cyt-c) into the nucleus, where it cooperates with the caspase family to initiate the cellular death program. Furthermore, mitochondria are calcium pumps that help the endoplasmic reticulum (ER) to regulate cellular calcium homeostasis (10), thus critically regulating cancer migration. Therefore, the roles of mitochondria in the regulation of cancer migration, apoptosis and metabolism have been well established. However, whether Mst1 can reduce NSCLC A549 cell viability by restricting mitochondrial function has yet to be fully elucidated.

F-actin is an important structural protein that is required for cellular cytoskeleton organization and cellular movement, and is also involved in processes including the regulation of cellular division, mitochondrial fission and filopodia formation (11). This affords F-actin a central position within cellular response networks. Based on previous studies, F-actin dysregulation is

associated with gastric cancer migration inhibition via sirtuin 1/mitofusin 2-mediated mitophagy (12,13). Furthermore, F-actin downregulation contributes to rectal cancer mitochondrial apoptosis via activation of the c-Jun N-terminal kinase (JNK)-dynamin-related protein 1-mitochondrial fission-HtrA serine peptidase 2/Omi axis (14). In cardiovascular disease, F-actin degradation promotes cardiac microvascular ischemia-reperfusion injury (11). Collectively, these findings confirmed that functional F-actin signaling is imperative to normal cell function. Notably, a relationship between Mst1 and F-actin has previously been established (6). Activated Mst1 has the ability to induce F-actin degradation, thus promoting apoptosis in endometriosis, colorectal cancer cell death and arrested liver cancer invasion. However, whether Mst1 has a critical role in NSCLC A549 cell survival via regulating F-actin homeostasis, invasion and metastasis remains to be elucidated.

At the molecular level, F-actin homeostasis is governed by Rho-associated coiled-coil containing protein kinase 1 (ROCK1) (15), which depolymerizes F-actin into G-actin. Furthermore, ample evidence has suggested the possibility of ROCK1 acting as a tumor suppressor in several types of cancer. Activated ROCK1 signaling promotes prostate cancer apoptosis by inducing cofilin-1 translocation onto the surface of mitochondria (16), whereas ROCK1 suppression accounts for renal cell carcinoma aggressiveness (17). Furthermore, overexpression of ROCK1 enhances myeloid leukemia apoptosis (18), inhibits osteosarcoma cell metastasis (19) and increases radiosensitization in pancreatic cancer (20). Taken together, these findings have established a central role for ROCK1 in suppressing cancer development and progression. However, whether ROCK1-mediated F-actin inactivation is regulated by Mst1 and is involved in NSCLC A549 cell migration, proliferation and apoptosis remains unclear. Therefore, the present study aimed to explore the role of Mst1 in the NSCLC A549 cell stress response, involving cancer cell mobility, death and growth, with a focus on ROCK1-mediated F-actin degradation and mitochondrial injury signaling.

Materials and methods

Cell culture and treatments. The normal pulmonary epithelial cell line BEAS-2B (American Type Culture Collection (ATCC)® no. CRL-9609™) and the NSCLC cell line A549 (ATCC® no. CCL-185EMT™) were purchased from ATCC (Manassas, VA, USA). The cells were cultured in Low Glucose-Dulbecco's modified Eagle's medium (L-DMEM; Gibco; Thermo Fisher Scientific, Inc., Waltham, MA, USA) containing low glucose, 10% fetal bovine serum (FBS; Gibco; Thermo Fisher Scientific, Inc.) and 1% streptomycin and penicillin at 37°C in an atmosphere containing 5% CO_2. To inhibit ROCK1 activity, Y-27632 (5 mM; cat. no. S1049; Selleck Chemicals, Houston, TX, USA) was added to the medium for 4 h (21).

Mst1 overexpression assay. The pDC315-Mst1 vector (1,336 bp; pDC315-Mst1-*Nhe*I-forward, 5'-CTAATGCGT TGCAATACGTGCGTCCTATATG-3' and pDC315-Mst1-*Hin*dIII-reverse, 5'-TTGTCCATTGCAAGGCCTCTGATT GAGTCTG-3') was designed and purchased from Shanghai GenePharma Co., Ltd. (Shanghai, China). Briefly, the plasmid (3.0 μg per 1x10^4 cells/well) was transfected into 293 cells

using Lipofectamine 2000® (Invitrogen; Thermo Fisher Scientific, Inc.). When the cells detached from the plates, the medium supernatant was collected (22). Subsequently, the viral supernatant was identified and was amplified by transfection into 293 cells three times, in order to obtain adenovirus (Ad)-Mst1, after which, Ad-Mst1 was transduced into the cells to induce overexpression of Mst1. A total of 1x10^5 cells/well were infected with 100 multiplicity of infection Ad-Mst1 or empty vector (Ad-ctrl) in Opti-MEM media (Gibco; Thermo Fisher Scientific, Inc.) for 6 h at 37°C, according to the manufacturer's protocol. Cells transduced with the Ad-ctrl were used as the control group (23).

Reactive oxygen species (ROS) detection via flow cytometry and immunofluorescence. Cellular ROS production was analyzed by flow cytometry, according to a previous study (24). Cells (1x10^6) were washed with cold PBS and cultured with the ROS probe dihydroethidium (1 mg/ml; Molecular Probes; Thermo Fisher Scientific, Inc.) at 37°C in the dark for 15 min. After the cells were washed three times with cold PBS, the cells were collected using 0.25% pancreatin. After resuspension in cold PBS, the cells were analyzed using a flow cytometer (BD FACSVerse; BD Biosciences, San Jose, CA, USA) and the data were analyzed with Flowmax software (Version 2.3; Sysmex Partec GmbH, Görlitz, Germany) (25). In addition, ROS was observed using a ROS probe. Cells (1x10^6) were loaded with the ROS probe dihydroethidium (5 mg/ml; Molecular Probes; Thermo Fisher Scientific, Inc.) in the dark for 10 min at room temperature. After washing with PBS, ROS production was monitored under an Olympus IX81 microscope (Olympus Corporation, Tokyo, Japan).

ATP production and mitochondrial potential. Cellular ATP generation was measured to reflect mitochondrial function. Firstly, A549 cells were washed three times with cold PBS at room temperature. Subsequently, a luciferase-based ATP assay kit (CellTiter-Glo® Luminescent Cell Viability Assay; cat. no. G7570; Promega Corporation, Madison, WI, USA) was used to analyze ATP content, according to the manufacturer's protocols (10). ATP production was measured using a microplate reader at a wavelength of 570 nm (Epoch 2; BioTek Instruments, Inc., Winooski, VT, USA) (26). To observe the mitochondrial potential, JC-1 staining (cat no. M34152; Thermo Fisher Scientific Inc.) was used. Briefly, 10 mg/ml JC-1 was added to the medium for 10 min at 37°C in the dark, in order to label mitochondria. Images were captured under an Olympus IX81 microscope (Olympus Corporation). Normal mitochondrial potential was indicated by red fluorescence, whereas damaged mitochondrial potential was indicated by green fluorescence (27).

Cell migration assay. For the cell migration assay, Transwell units (Corning Incorporation, Corning, NY, USA) with an 8-μm pore size polycarbonate filter were used. A549 cells were initially transduced with Ad-Mst1 and were then isolated using 0.25% trypsin. Trypsin-mediated digestion and isolation was conducted to remove apoptotic cells. To further exclude the influence of cell apoptosis on the Transwell assay, a lactate dehydrogenase (LDH) release assay was used to evaluate cell viability. Subsequently, ~1x10^5 cells were seeded in the upper chamber of the Transwell units; the lower chamber was filled with 600 μl L-DMEM supplemented with 1% FBS (Gibco;

Thermo Fisher Scientific, Inc.). Following a 12-h incubation at 37˚C, the medium was removed and the cells were fixed with 3.7% paraformaldehyde for ~10 min at room temperature (28). The cells in the upper chamber were removed using a cotton swab, and the migrated cells were stained with 0.1% crystal violet for 15 min at room temperature. Subsequently, the samples were observed under a digital microscope system (IX81; Olympus Corporation). The images were captured and the number of migrated cells was recorded in at least five fields.

LDH assay and caspase-9 activity detection. LDH is released into the medium when cellular membranes rupture. To evaluate the levels of LDH in the medium, an LDH Release Detection kit (Beyotime Institute of Biotechnology, Haimen, China) was used according to the manufacturer's protocol. To analyze alterations in caspase-9, a caspase-9 activity kit (cat no. C1158; Beyotime Institute of Biotechnology) was conducted, according to the manufacturer's protocol (29). Briefly, to measure caspase-9 activity, 5 μl LEHD-p-NA substrate (4 mM, 200 μM final concentration) was added to the samples for 1 h at 37˚C. Subsequently, the absorbance was recorded at 400 nm using a microplate reader, in order to reflect caspase-9 activities (30).

Glutathione (GSH), GSH peroxidase (GPX) and superoxide dismutase (SOD) detection, mitochondrial respiratory complex activity estimation, lactate production measurement and glucose uptake evaluation. GSH (cat. no. T10095; Thermo Fisher Scientific Inc.), GPX (cat. no. S0056; Beyotime Institute of Biotechnology) and SOD (cat. no. BMS222TEN; Thermo Fisher Scientific Inc.) levels were measured, according to the manufacturers' protocols, using a microplate reader (Epoch 2; BioTek Instruments, Inc.) (31). Mitochondrial respiratory complex activity was estimated using commercially available kits (cat. nos. ab109721 and ab109878; Abcam, Cambridge, MA, USA) according to the manufacturer's protocols. To analyze lactate production, a lactate assay kit (cat. no. K607-100; BioVision, Inc.) was used, according to a previous study (32). In addition, cellular glucose uptake was evaluated using a glucose absorption assay kit (cat. no. K606-100; BioVision, Inc.), according to the manufacturer's protocol (33).

Western blotting. Cells were lysed in radioimmunoprecipitation assay lysis buffer (Beyotime Institute of Biotechnology). Total protein was analyzed using the bicinchoninic acid assay (Beyotime Institute of Biotechnology) and 70 μg lysates were separated by 10-15% SDS-PAGE, and proteins were electrotransferred onto Pure Nitrocellulose Blotting membranes (EMD Millipore, Billerica, MA, USA). The membranes were then blocked with 5% non-fat milk for 2 h at room temperature (34) and were washed with Tris-buffered saline-0.1% Tween (TBST). The membranes were then incubated with the following primary antibodies: Caspase-9 (1:1,000; cat. no. ab32539; Abcam), pro-caspase-3 (1:1,000; cat. no. ab13847; Abcam), cleaved caspase-3 (1:1,000; cat. no. ab49822; Abcam), B-cell lymphoma 2 (Bcl2; 1:1,000; cat. no. 3498; Cell Signaling Technology, Inc.), Bcl2-associated death promoter (Bad; 1:1,000; cat. no. 9292; Cell Signaling Technology, Inc.), cellular inhibitor of apoptosis protein (c-IAP; 1:1,000; cat. no. 4952; Cell Signaling Technology, Inc.), Mst1 (1:1,000; cat. no. 3682; Cell Signaling Technology,

Inc.), F-actin (1:1,000; cat. no. ab205; Abcam), complex III subunit core 2 (CIII-core2; 1:1,000; cat. no. 459220; Invitrogen; Thermo Fisher Scientific, Inc.), complex II (CII-30; 1:1,000; cat. no. ab110410; Abcam), C-X-C chemokine receptor type (CXCR)4 (1:1,000; cat. no. ab1670; Abcam), CXCR7 (1:1,000; cat. no. ab38089; Abcam), cyclin D1 (1:1,000; cat. no. ab16663; Abcam), cyclin E (1:1,000; cat. no. ab33911; Abcam), cyt-c (1:1,000; cat. no. ab90529; Abcam) and ROCK1 (1:1,000; cat. no. ab45171; Abcam) at 4˚C overnight. After washing with TBST, the membranes were incubated with horseradish peroxidase-coupled secondary antibodies (1:2,000; cat. nos. 7074 and 7076; Cell Signaling Technology, Inc.) for 1 h at room temperature. The proteins were visualized using Pierce enhanced chemiluminescence western blotting substrate (Pierce; Thermo Fisher Scientific, Inc.) and autoradiography. Subsequently, the blots were analyzed using Quantity One 4.6 software (Bio-Rad Laboratories, Inc., Hercules, CA, USA). GAPDH (1:1,000; cat. no. 5174; Cell Signaling Technology, Inc.), β-actin (1:1,000; cat. no. 4970; Cell Signaling Technology, Inc.) and translocase of the outer membrane 20 (1:1,000; cat. no. ab56783; Abcam) were used as internal controls (35).

Isolation of mitochondria-enriched fraction. Mitochondrial and cytoplasmic cyt-c expression was measured via isolation of the mitochondrial-enriched fraction, followed by western blotting. After isolation of mitochondria-enriched fraction, the remaining fraction was used to analyze cytoplasmic protein expression. In order to isolate the mitochondria-enriched fraction, cells were washed with cold PBS and were scraped; the homogenates were then centrifuged at 800 x g for 5 min at 4˚C. The supernatants were centrifuged at 10,000 x g for 20 min at 4˚C to acquire pellets, which were spun again. The final pellets were suspended in lysis buffer (cat. no. P0013E; Beyotime Institute of Biotechnology) containing 1% Triton X-100 and were noted as mitochondrial-rich lysate fractions.

Terminal deoxynucleotidyl transferase-mediated dUTP nick end labeling (TUNEL). Apoptotic cells were detected using an In Situ Cell Death Detection kit (cat. no. C10245; Thermo Fisher Scientific Inc.), according to the manufacturer's protocol. Briefly, cells (1x10⁶) were fixed with 4% paraformaldehyde at 37˚C for 15 min. Blocking buffer (3% H_2O_2 in CH_3OH) was added to the wells, and cells were then permeabilized with 0.1% Triton X-100 in 0.1% sodium citrate for 2 min on ice. Finally, the cells were incubated with TUNEL reaction mixture for 1 h at 37˚C. DAPI (Sigma-Aldrich; Merck KGaA, Darmstadt, Germany) was used to counterstain the nuclei, and the numbers of TUNEL-positive cells were recorded (36) under a digital microscope system (IX81; Olympus Corporation).

5-ethynyl-2'-deoxyuridine (EdU) incorporation assay and MTT experiments. The EdU incorporation assay was performed using an EdU kit (cat. no. A10044; Thermo Fisher Scientific Inc.) (37). Briefly, EdU (2 nM/well) was diluted in complete culture medium, and the cells (1x10⁶) were incubated with the dilution for 2 h at 37˚C. Subsequently, the cells were fixed with 4% paraformaldehyde for 15 min at 37˚C and were incubated with Apollo Staining reaction liquid for 30 min. DAPI was used to counterstain the nuclei for 15 min at room temperature under a digital microscope system (IX81; Olympus Corporation).
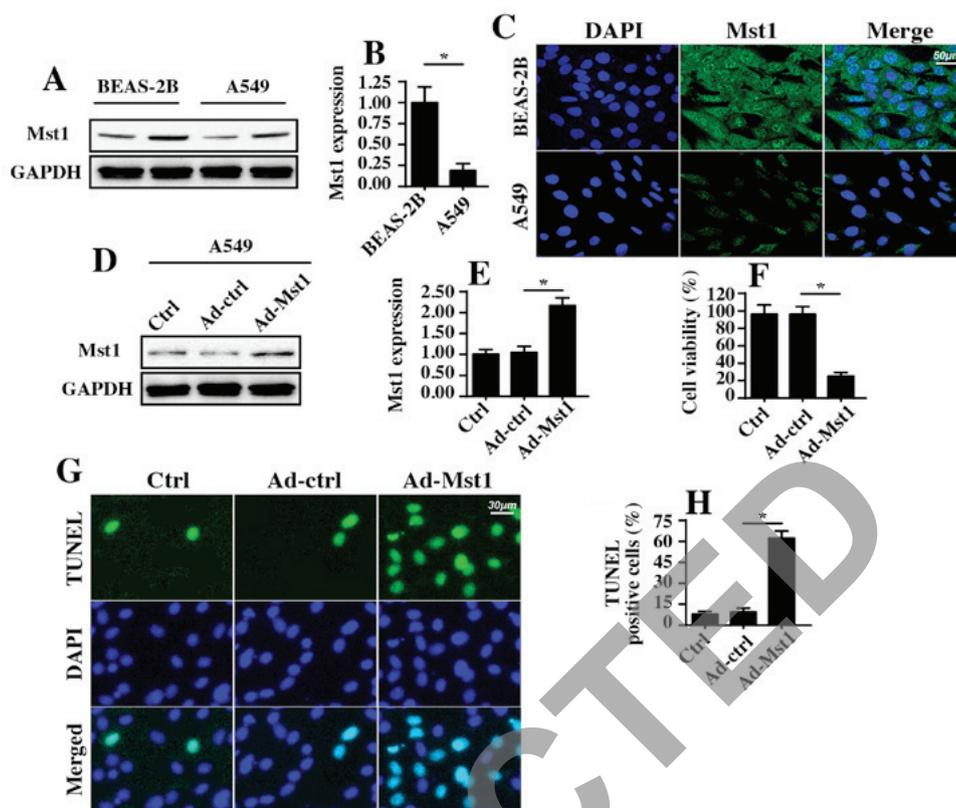
Figure 1. Mst1 is downregulated in A549 cells and regulates A549 cell apoptosis. (A and B) Western blotting was used to analyze the protein expression levels of Mst1 in the normal pulmonary epithelial cell line BEAS-2B and in A549 cells. (C) Immunofluorescence analysis of Mst1; DAPI used to label the nuclei. (D and E) Mst1 overexpression was performed via Ad-Mst1 transduction. Western blotting was used to evaluate the protein expression levels of Mst1 in response to Ad-Mst1 transduction. (F) MTT assay was used to analyze cell viability following Ad-Mst1 transduction. (G and H) TUNEL assay was used to quantify the cellular apoptotic rate. The number of TUNEL-positive cells was recorded. *P<0.05. Ad, adenovirus; Mst1, mammalian STE20-like kinase 1; TUNEL, terminal deoxynucleotidyl transferase-mediated dUTP nick end labeling.

MTT was used to analyze cellular viability. A549 cells ($1x10^6$ cells/well) were cultured on a 96-well plate at 37°C in an atmosphere containing 5% CO_2, with or without Ad-Mst1 transduction. Subsequently, 40 μl MTT solution (2 mg/ml; Sigma-Aldrich; Merck KGaA) was added to the medium for 4 h at 37°C in an atmosphere containing 5% CO_2. Subsequently, the cell medium was discarded, and 80 μl dimethyl sulfoxide was added to the wells for 1 h at 37°C in an atmosphere containing 5% CO_2 in the dark. The optical density (OD) of each well was observed at an absorbance of 490 nm via a spectrophotometer (Epoch 2; BioTek Instruments, Inc.) (38).

Immunofluorescence confocal microscopy. The cells ($1x10^6$) were washed twice with PBS and permeabilized in 0.1% Triton X-100 overnight at 4°C. Subsequently, 10% goat serum albumin (Invitrogen; Thermo Fisher Scientific, Inc.) was used to block the samples for 1 h at room temperature. The sections were then cryoprotected in a PBS solution supplemented with 0.9 mol/l sucrose overnight at 4°C. Following neutralization with NH_4Cl buffer, the sections were permeabilized for 45 min with 0.05% saponin/PBS (pH 7.4) and incubated with H_2O_2 (3%) for 10 min Subsequently, samples were treated overnight at 4°C with the following primary antibodies: Cyt-c (1:500; cat. no. ab90529; Abcam), Mst1 (1:200; cat. no. 3682; Cell Signaling Technology, Inc.), F-actin (1:1,000; cat. no. ab205; Abcam), cyclin D1 (1:500; cat. no. ab16663; Abcam) and cyclin E (1:500; cat. no. ab33911; Abcam). After

three rinses in PBS, secondary antibodies (Alexa Fluor® 488 donkey anti-rabbit antibody; 1:1,000; cat. no. A-21206 and Alexa Fluor® Plus 647 goat anti-rabbit antibody; 1:1,000; cat. no. A-32733; Invitrogen; Thermo Fisher Scientific, Inc.) were added to the samples for 1 h at room temperature. The samples were stained with DAPI (10 nM) for 5 min. Confocal immunofluorescence images were captured using FV10-ASW 1.7 software and an Olympus IX81 microscope (Olympus Corporation) (39). The length of filopodia formation was measured using Image-Pro Plus 6.0 (Media Cybernetics, Rockville, MD, USA).

Statistical analysis. Experiments were repeated three times and data are expressed as the means ± standard error of the mean. Statistical analyses were performed using one-way analysis of variance followed by a Bonferroni post hoc test. P<0.05 was considered to indicate a statistically significant difference. Statistical analysis was performed using GraphPad Prism 5.0 (GraphPad Software, Inc., La Jolla, CA, USA).

Results

Mst1 is downregulated in NSCLC A549 cells, and overexpression of Mst1 promotes A549 cell apoptosis. To address the functional role of Mst1 in the phenotypic alterations of A549 cells, western blotting was used to examine the protein expression levels of Mst1 in A549 cells. As shown in Fig. 1A
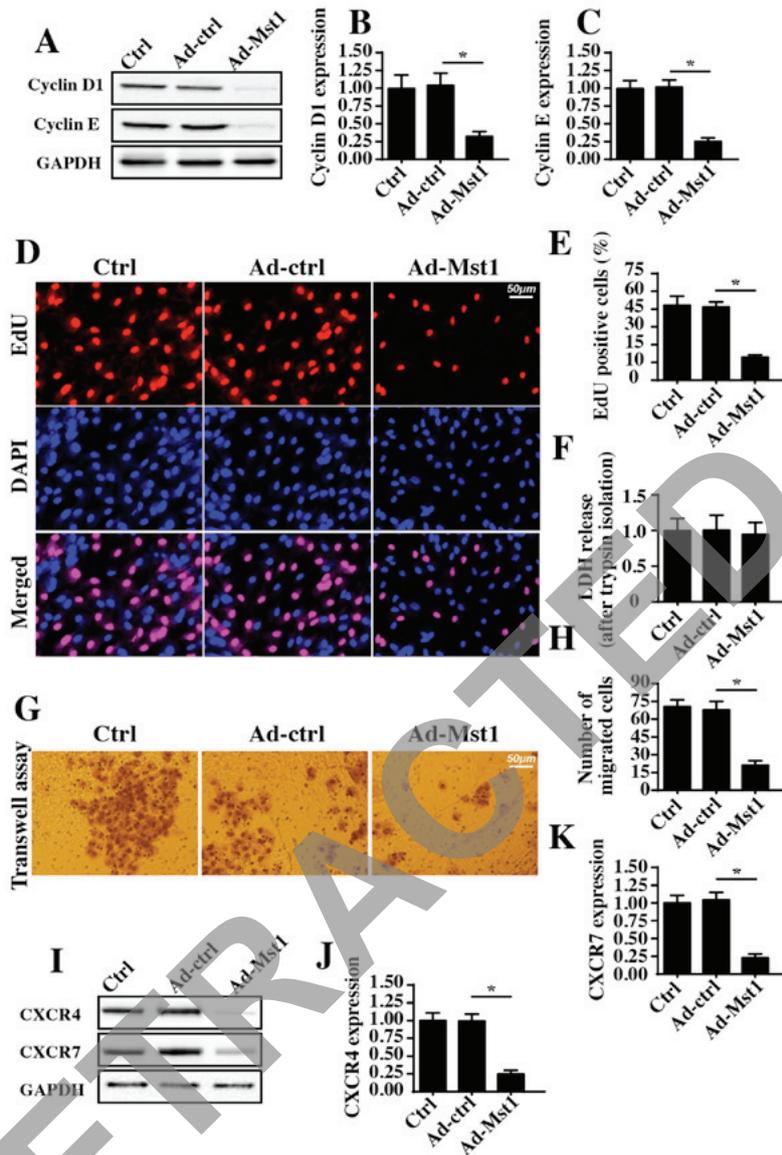
Figure 2. Mst1 affects A549 cell migration and proliferation. (A-C) Expression levels of proliferation-associated proteins were analyzed by western blotting in A549 cells following Ad-Mst1 transduction. (D and E) Cell proliferation was measured via EdU staining. The number of EdU-positive cells was recorded. (F) A549 cells transduced with Ad-Mst1 were isolated using 0.25% trypsin and cell viability was determined using a LDH release assay. (G and H) Isolated cells were seeded onto Transwell units and a Transwell assay was performed to evaluate cell migration; the number of migrated cells was recorded. (I-K) Chemokines CXCR4 and CXCR7 were measured via western blotting in response to Ad-Mst1 transduction. *P<0.05. Ad, adenovirus; CXCR, C-X-C chemokine receptor; EdU, 5-ethynyl-2'-deoxyuridine; LDH, lactate dehydrogenase; Mst1, mammalian STE20-like kinase 1.

and B, abundant Mst1 expression was observed in the normal pulmonary epithelial cell line BEAS-2B. In comparison, Mst1 expression was markedly reduced in A549 cells; these findings were further supported by immunofluorescence staining (Fig. 1C). These results indicated that Mst1 expression may be downregulated in A549 cells. Subsequently, Mst1 was overexpressed in A549 cells via an adenovirus-based Mst1 overexpression method. Transduction efficiency is shown in Fig. 1D and E, as determined by western blotting. Following overexpression of Mst1, cellular viability and apoptosis were analyzed. MTT assays revealed that Mst1 overexpression in A549 cells significantly reduced cellular viability (Fig. 1F). In agreement with these results, the cellular apoptotic rate, as measured by TUNEL staining (Fig. 1G and H), revealed that the number of TUNEL-positive apoptotic cells was significantly increased in response to Ad-Mst1 transduction

compared with in the control group. These results suggested that Mst1 may function as a tumor suppressor in A549 cells by promoting cancer cell apoptosis.

Overexpression of Mst1 reduces A549 cell proliferation and migration. The present study further investigated the effects of Mst1 overexpression on the growth and metastasis of A549 cells. Initially, cyclin D1 and cyclin E expression levels, which were detected by western blotting, were significantly decreased in response to Mst1 overexpression compared with in the control group (Fig. 2A-C). As cyclin D1 and cyclin E interact with each other and generate cyclin-dependent kinase (Cdk)4/6-cyclin D and/or Cdk2-cyclin E complexes, which accelerate transition from the G0/G1 to S stage, the present study aimed to determine whether Mst1 overexpression augmented the number of cancer cells at S stage. Through EdU staining, which labels
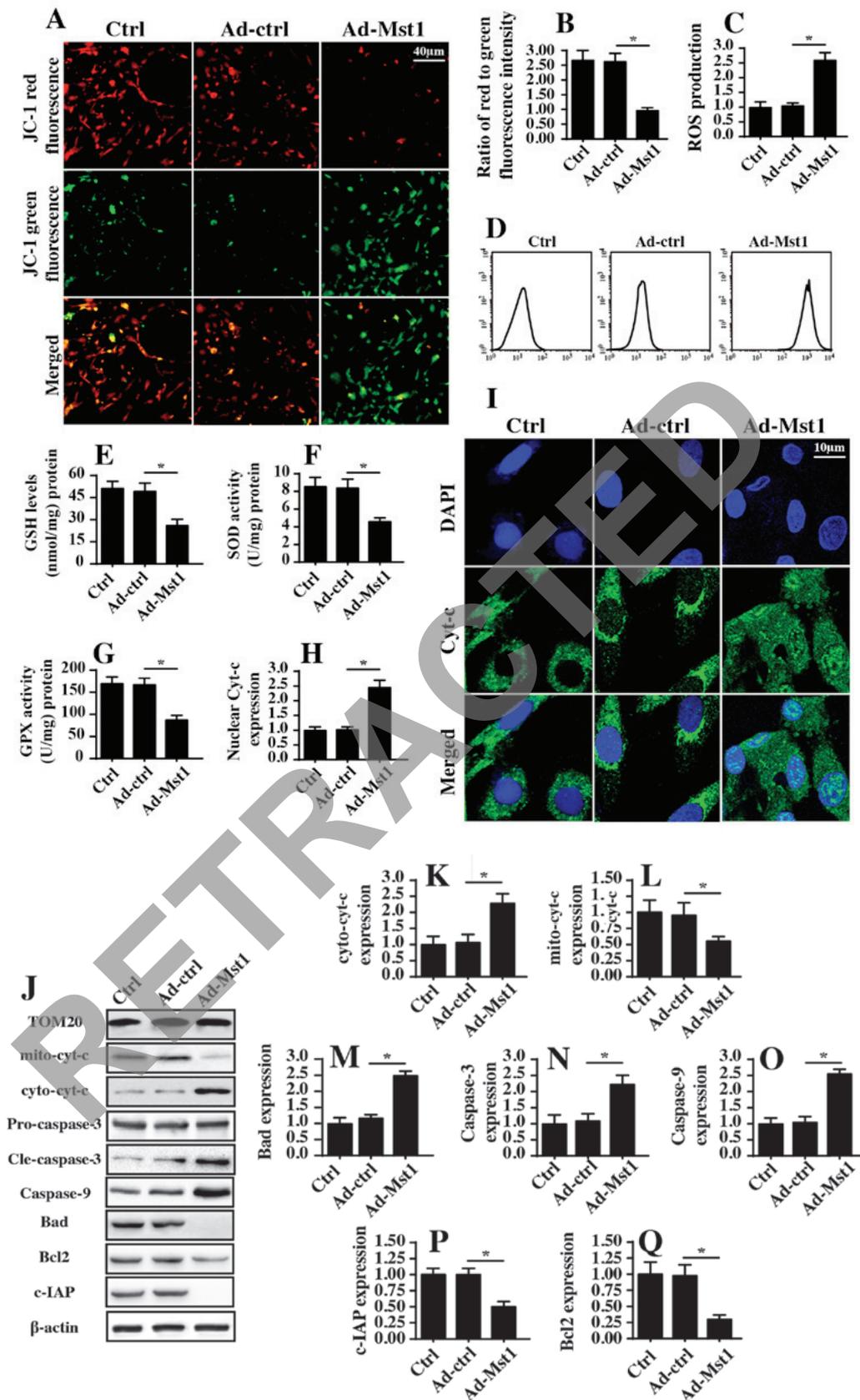
Figure 3. Mst1 overexpression is associated with mitochondrial damage. (A and B) Mitochondrial potential was observed via JC-1 staining. Red fluorescence indicated normal mitochondrial potential, whereas green fluorescence indicated damage to mitochondrial potential. (C and D) ROS production was measured by flow cytometry. Ad-Mst1 transduction increased the ROS content in A549 cells. (E-G) Antioxidants were detected by ELISA. (H and I). Cyt-c translocation into the nucleus was observed by co-staining cells with cyt-c and DAPI. (J-Q) Western blotting of proteins associated with mitochondrial apoptosis. The expression levels of pro-apoptotic and anti-apoptotic proteins were analyzed by western blotting. TOM20 was used as a loading control for mito cyt-c expression. *P<0.05. Ad, adenovirus; Bad, Bcl2-associated death promoter; Bcl2, B-cell lymphoma 2; c-IAP, cellular inhibitor of apoptosis protein; cyt-c, cytochrome *c*; GPX, GSH peroxidase; GSH, glutathione; mito, mitochondrial; Mst1, mammalian STE20-like kinase 1; ROS, reactive oxygen species; SOD, superoxide dismutase; TOM20, translocase of the outer membrane 20.
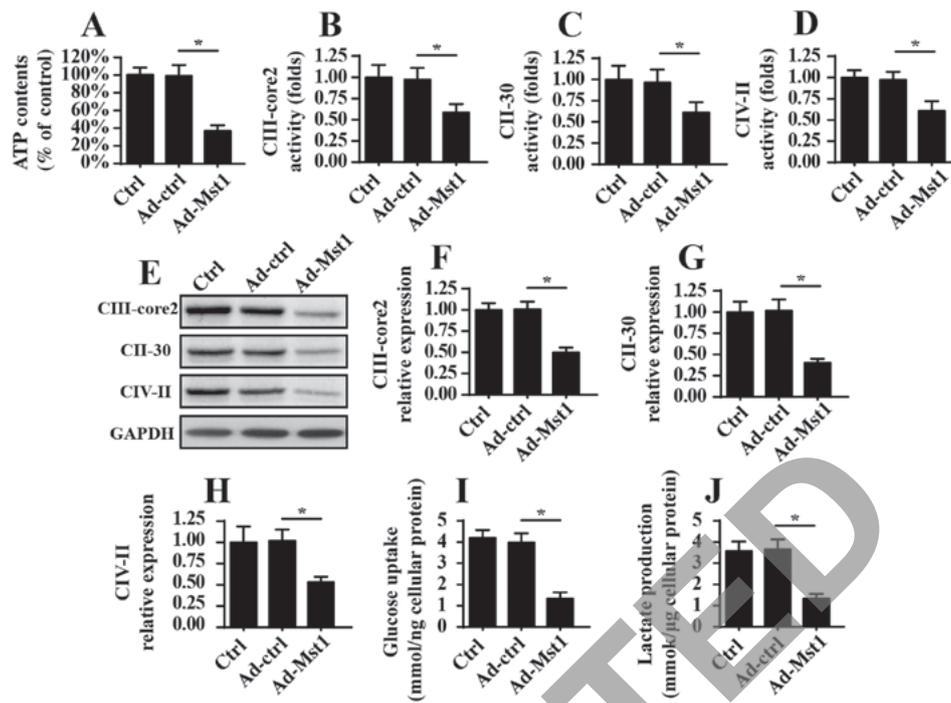
Figure 4. Mst1 overexpression suppresses mitochondrial respiratory function. (A) ATP production was measured in A549 cells following Ad-Mst1 transduction. (B-D) Mitochondrial respiratory complex protein activity was evaluated via ELISA analyses. Ad-Mst1 transduction decreased the activity of mitochondrial respiratory complex proteins in A549 cells. (E-H) Western blotting was used to analyze the protein expression levels of mitochondrial respiratory complexes. GAPDH was used as a loading control for western blotting. (I and J) Glucose uptake and lactate production were measured in the medium following Ad-Mst1 transduction. *P<0.05. Ad, adenovirus; CII-30, complex II; CIII-core2, complex III subunit core 2; CIV-II, complex IV subunit II; Mst1, mammalian STE20-like kinase 1.

cells at S stage, it was demonstrated that Ad-Mst1 transduction markedly decreased the ratio of EdU-positive cells compared with in the control group (Fig. 2D and E). Therefore, these findings indicated that Mst1 affects A549 cell proliferation.

The present study also observed cellular migration in response to Mst1 overexpression. To exclude the influence of cell viability on the Transwell assay, A549 cells transduced with Ad-Mst1 were isolated using 0.25% trypsin. Subsequently, a LDH release assay was used to evaluate cell viability following trypsin isolation. The present results demonstrated that there was no significant difference in cell viability in the Ad-Mst1 and Ad-ctrl groups (Fig. 2F). Subsequently, a Transwell assay was conducted. The number of migrated cells was decreased in response to Mst1 overexpression (Fig. 2G and H). Furthermore, the expression levels of the chemotactic factors CXCR4 and CXCR7 were detected. Notably, the expression levels of CXCR4 and CXCR7 were downregulated following Ad-Mst1 transduction (Fig. 2I-K), thus suggesting that Mst1 overexpression suppressed A549 cell migration. Collectively, these results demonstrated that overexpression of Mst1 inhibited A549 cell growth and metastasis *in vitro*.

Overexpression of Mst1 activates the mitochondrial apoptotic pathways. Recent studies (40,41) have indicated that mitochondrial dysfunction is associated with cancer cell apoptosis, inhibition of migration and proliferation arrest via numerous mechanisms. Therefore, the present study measured mitochondrial function in A549 cells with or without Mst1 overexpression. Initially, mitochondrial potential was evaluated by JC-1 staining. Compared with in the control group, Mst1 overexpression reduced mitochondrial potential (Fig. 3A and B), as evidenced

by reduced red fluorescence and increased green fluorescence. In response to mitochondrial potential collapse, excessive electrons would be released from the mitochondrial respiratory complex, thus promoting ROS production, which induces oxidative stress in cancer cells. Based on this information, cellular ROS was measured by flow cytometry. Compared with in the control group, Mst1 overexpression enhanced ROS production (Fig. 3C and D). In response to increased ROS, cellular antioxidant factors, including GSH, SOD and GPX, were markedly downregulated in response to Mst1 overexpression (Fig. 3E-G). Furthermore, excessive ROS has the ability to promote mitochondrial pro-apoptotic factor translocation into the nucleus. Through immunofluorescence assays, it was revealed that Mst1 overexpression induced cyt-c release from the mitochondria into the nucleus compared with in the control group (Fig. 3H and I). These findings were further supported by western blotting (Fig. 3J-L). Furthermore, Mst1 overexpression upregulated the expression levels of mitochondrial pro-apoptotic proteins (Bad, caspase-9 and caspase-3) and downregulated the expression levels of anti-apoptotic factors (c-IAP and Bcl2) (Fig. 3J-Q). Collectively, these findings indicated that Mst1 overexpression may activate mitochondrial apoptosis in A549 cells.

Overexpression of Mst1 induces mitochondrial energy disorder. As well as their involvement in mitochondrial apoptosis, mitochondria are the center of cellular ATP production, which provides enough energy to sustain cancer cell growth and mobilization. The present study aimed to investigate the role of Mst1 in mitochondrial metabolism. Initially, ATP production was measured in A549 cells; the results indicated that Mst1 overexpression suppressed ATP production (Fig. 4A).
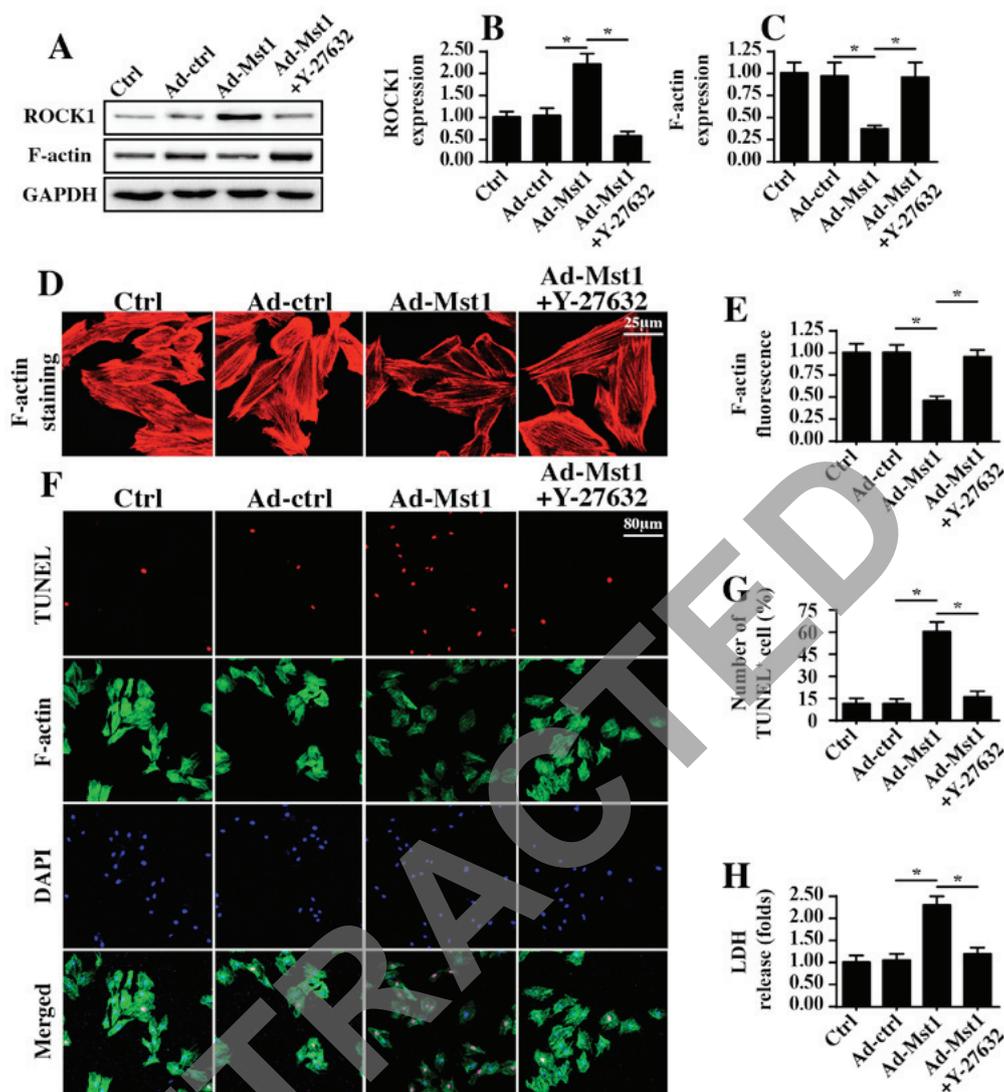
Figure 5. ROCK1/F-actin pathways are regulated by Mst1 and contribute to A549 cell apoptosis. (A-C) Western blotting was performed to analyze the protein expression levels of ROCK1 and F-actin. (D and E) Immunofluorescence of F-actin in response to treatment with Y-27632, which is an inhibitor of the ROCK1 pathway that was used to inhibit ROCK1 activation. Suppression of ROCK1 attenuated F-actin expression. (F and G) Staining of TUNEL-positive cells and F-actin. More TUNEL-positive cells were associated with decreased F-actin expression. (H) LDH release assay was used to evaluate the pro-apoptotic effects of Mst1. *P<0.05. Ad, adenovirus; LDH, lactate dehydrogenase; Mst1, mammalian STE20-like kinase 1; ROCK1, Rho-associated coiled-coil containing protein kinase 1; TUNEL, terminal deoxynucleotidyl transferase-mediated dUTP nick end labeling.

Since ATP production is dependent on the activity and expression of the mitochondrial respiratory complex, this study aimed to determine whether Mst1 affected the activity and expression of the mitochondrial respiratory complex. Through ELISA analyses, it was revealed that mitochondrial respiratory complex activity was decreased in response to Ad-Mst1 transduction (Fig. 4B-D). Furthermore, the protein expression levels of the mitochondrial respiratory complexes, as measured by western blotting, were predominantly suppressed by Mst1 overexpression (Fig. 4E-H). Collectively, these data indicated that Mst1 impaired mitochondrial respiration and induced energy disorder. To provide more solid evidence for the role of Mst1 in cellular energy metabolism, the present study analyzed glucose and lactate content in the medium following Ad-Mst1 transduction. As shown in Fig. 4I and J, Mst1 overexpression interrupted glucose consumption and thus reduced the production of lactate, which is indicative of the termination

of glycometabolism. Therefore, these data indicated that Mst1 overexpression may suppress mitochondrial energy metabolism in A549 cells.

ROCK1/F-actin signaling pathways are activated by Mst1. To determine the underlying mechanism by which Mst1 regulates mitochondrial damage and energy disorder, this study focused on the ROCK1/F-actin axis, since ROCK1/F-actin pathways have been revealed to be the upstream regulatory molecules for mitochondrial damage in several types of cancer cell (42,43). Through western blotting, it was demonstrated that Mst1 overexpression enhanced the protein expression levels of ROCK1, which was followed by a decrease in F-actin expression (Fig. 5A-C). Subsequently, a ROCK1 loss-of-function assay was conducted via administration of Y-27632 after Ad-Mst1 transduction, which is an inhibitor of ROCK1. Following application of Y-27632 in Mst1-overexpressed
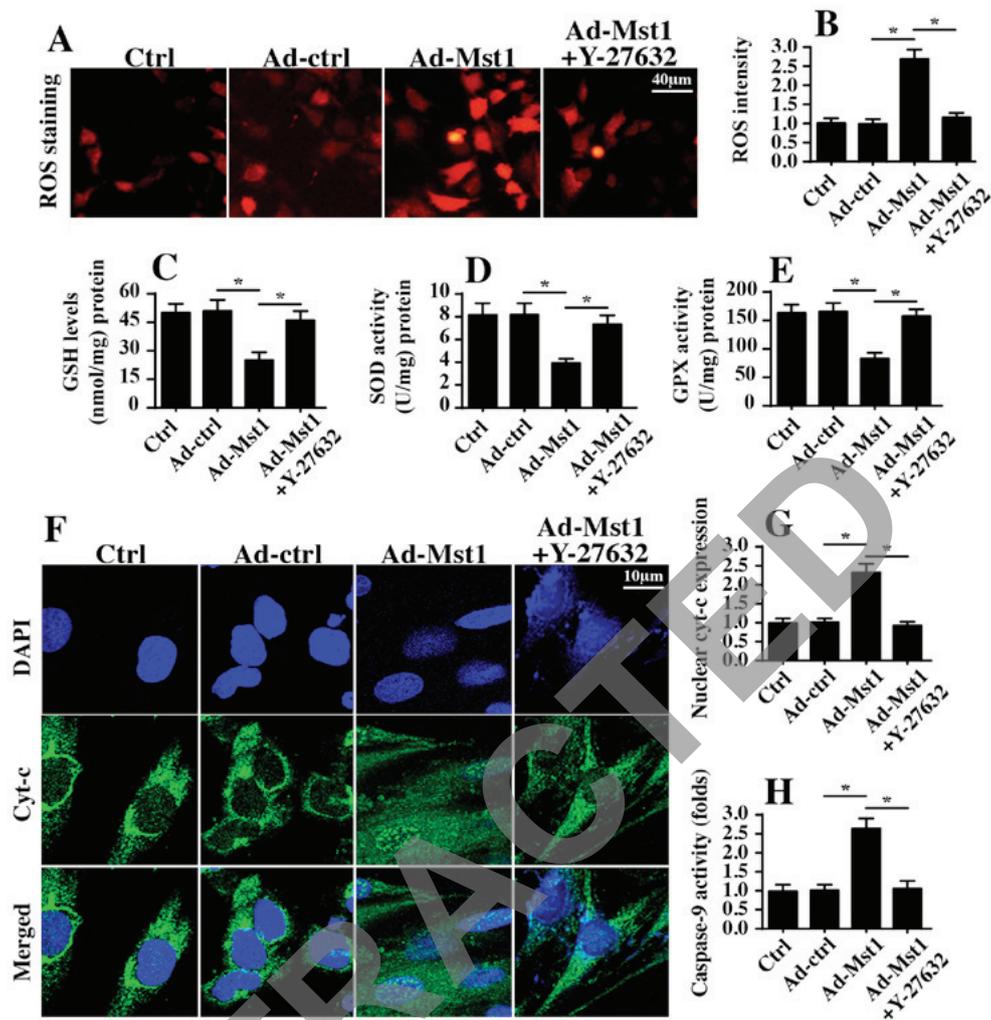
Figure 6. Rho-associated coiled-coil containing protein kinase 1/F-actin pathways modulate mitochondrial function. (A and B) ROS staining was used to analyze cellular oxidative stress. Ad-Mst1-mediated ROS overproduction was significantly suppressed by Y-27632. (C-E) Antioxidant factors were evaluated via ELISA. (F and G) Cyt-c translocation into the nucleus was observed by co-staining cells with cyt-c and DAPI. (H) Caspase-9 activity was measured via ELISA. Mst1-mediated casapse-9 activation was inhibited by Y-27632 in A549 cells. *P<0.05. Ad, adenovirus; cyt-c, cytochrome *c*; GPX, GSH peroxidase; GSH, glutathione; Mst1, mammalian STE20-like kinase 1; ROS, reactive oxygen species; SOD, superoxide dismutase.

cells, ROCK1 expression was reduced (Fig. 5A-C), whereas F-actin expression was increased. These findings were further supported by immunofluorescence assays, which indicated that Mst1 overexpression induced the degradation of F-actin, whereas this effect was reversed by Y-27632 administration (Fig. 5D and E). Based on these results, it may be suggested that Mst1 overexpression has the ability to activate ROCK1 expression and thus reduce F-actin stabilization.

In order to observe whether ROCK1/F-actin was involved in Mst1-mediated A549 cell apoptosis, F-actin staining and TUNEL assays were performed. Compared with in the control group, Mst1 overexpression augmented the number of TUNEL-positive cells, which was accompanied by a drop in the fluorescence intensity of F-actin (Fig. 5F and G). However, Mst1-induced cell apoptosis and F-actin degradation were reversed by Y-27632 (Fig. 5F and G). This finding was further supported by an LDH release assay (Fig. 5H), which indicated that Mst1-mediated LDH release could be reversed by Y-27632 treatment. Collectively, these observations indicated that Mst1 may regulate A549 cell apoptosis via the ROCK1/F-actin pathway.

The Mst1/ROCK/F-actin axis regulates mitochondrial injury. Since mitochondria are potential targets of Mst1 and impact A549 cell viability, the present study aimed to determine whether mitochondrial homeostasis was regulated by the Mst1/ROCK/F-actin axis. To verify the hypothesis, ROS production was initially detected, which is an early indicator of mitochondrial damage. Consistent with the aforementioned findings, Mst1 overexpression augmented ROS generation, as assessed by ROS staining (Fig. 6A and B). However, inhibition of ROCK1 pathways via Y-27632 significantly suppressed ROS production despite transduction with Ad-Mst1 (Fig. 6A and B). Furthermore, inhibition of ROCK1 blocked the pro-oxidant effects of Mst1, and the contents of SOD, GSH and GPX were recovered in A549 cells (Fig. 6C-E). In addition, Mst1-mediated cyt-c translocation into the nucleus was disrupted by Y-27632 administration (Fig. 6F and G). These findings indicated that the ROCK1/F-actin axis may be required for Mst1-associated mitochondrial apoptosis. To provide more solid evidence to explain the role of the ROCK1/F-actin axis in mitochondrial damage, caspase-9 activity, which
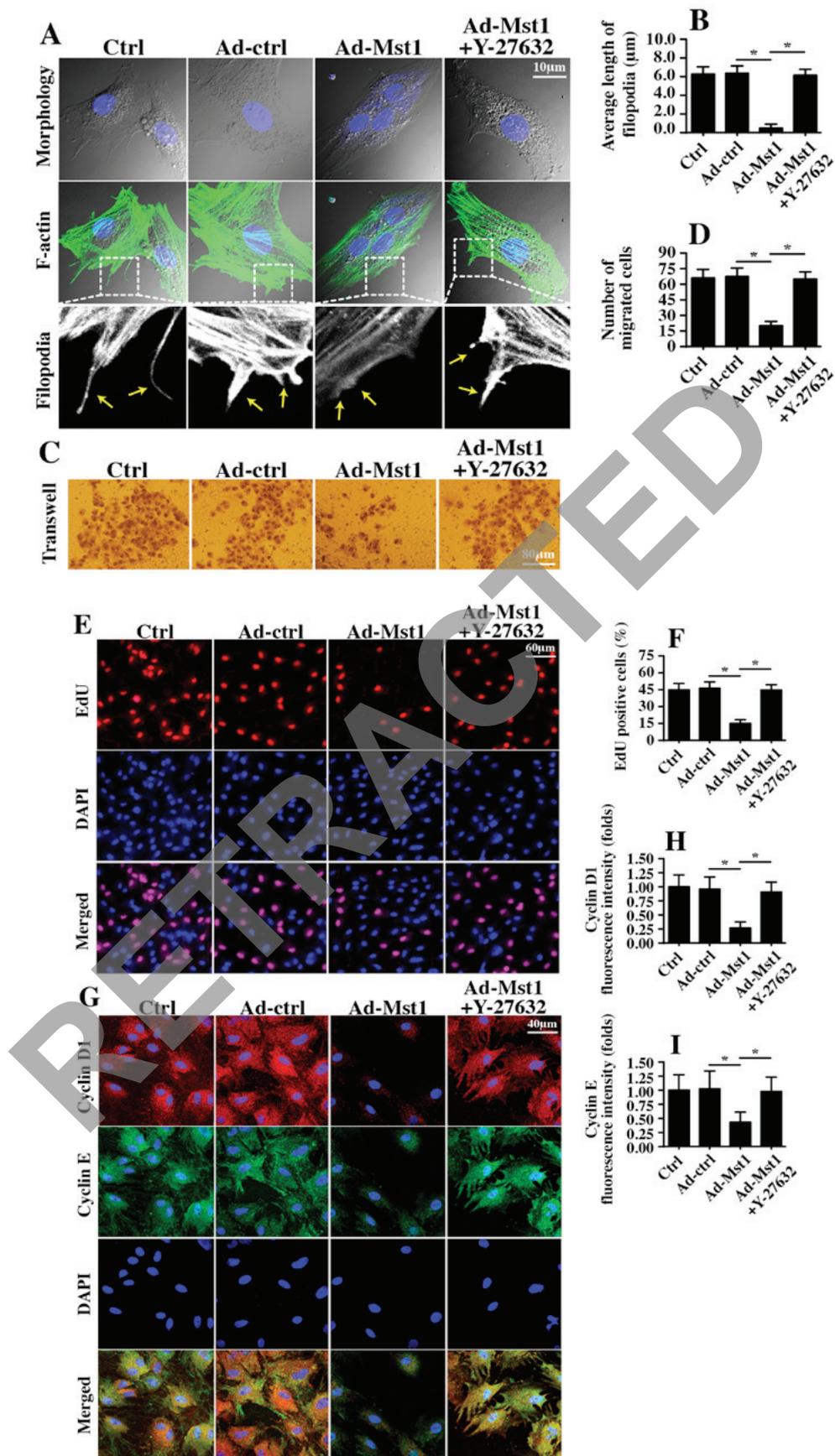
Figure 7. Mst1-Rho-associated coiled-coil containing protein kinase 1-F-actin pathways control A549 cell migration and proliferation. (A and B) Immunofluorescence analysis of F-actin. The average length of filopodia was measured in response to Ad-Mst1 transduction and Y-27632 treatment. (C and D) Transwell assay was conducted on A549 cells following Ad-Mst1 transduction and Y-27632 administration. (E and F) EdU assay was used to observe cellular proliferation. The number of EdU-positive cell was recorded. (G-I) Immunofluorescence analysis of cyclin proteins. Cyclin E and cyclin D1 were observed and the fluorescence intensity was measured in response to Ad-Mst1 transduction and Y-27632 treatment. *P<0.05. Ad, adenovirus; EdU, 5-ethynyl-2'-deoxyuridine; Mst1, mammalian STE20-like kinase 1.
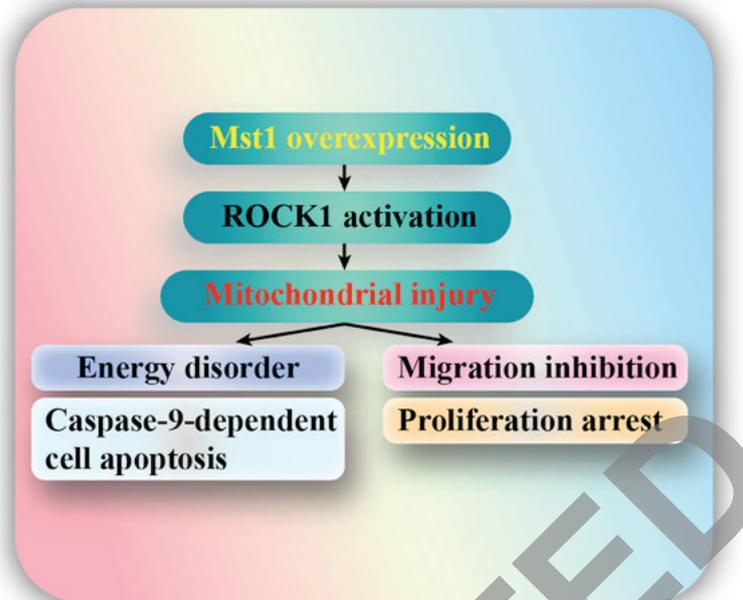
Figure 8. Mst1 overexpression promoted mitochondrial injury, as evidenced by reduced mitochondrial potential, uncontrolled oxidative stress, increased pro-apoptotic protein translocation, reduced mitochondrial energy metabolism and activated caspase-9 signals. Furthermore, Mst1 overexpression impaired migration and reduced proliferation in A549 cells. Mst1, mammalian STE20-like kinase 1; ROCK1, Rho-associated coiled-coil containing protein kinase 1.

is a hallmark of mitochondrial death, was measured via ELISA. Compared with in the control group, Mst1 overexpression elevated caspase-9 activity (Fig. 6H); however, this effect was reversed by Y-27632. Taken together, these data suggested that the ROCK1/F-actin axis may be activated by Mst1 and could contribute to mitochondrial injury in A549 cells.

Mst1/ROCK1/F-actin pathways are involved in A549 cell migration inhibition and proliferation arrest. Finally, the present study aimed to determine whether the ROCK/F-actin pathway is necessary for Mst1-mediated A549 cell migration inhibition and proliferation arrest. Therefore, filopodia formation was observed; filopodia is the major vehicle for cellular migration. Mst1 overexpression hampered filopodia formation, as evidenced by shorter and fewer filopodia outside of the cellular membrane (Fig. 7A and B). Conversely, this conformational alteration was reversed by Y-27632 (Fig. 7A and B). Furthermore, Transwell assays revealed that the number of migrated cells was reduced in response to Mst1 overexpression but reverted to normal levels following ROCK1 suppression (Fig. 7C and D). These findings indicated that the ROCK1/F-actin pathway was responsible for Mst1-mediated A549 cell migration inhibition.

The EdU assay was used to observe cell growth. Similar to the aforementioned results, Mst1 overexpression reduced the number of EdU-positive cells, whereas this effect was reversed by Y-27632 (Fig. 7E and F). Furthermore, through immunofluorescence analysis, it was revealed that Mst1-inhibited cyclin D1/E expression was rescued by Y-27632 (Fig. 7G-I). These findings indicated that Mst1 suppressed A549 cell proliferation by regulating the ROCK1/F-actin pathway.

Discussion

Lung cancer is currently one of the leading causes of cancer-associated mortality for older patients. Despite advances in its early diagnosis and treatment, additional investigations elucidating the mechanism underlying tumor progression are clinically required due to the high prevalence, invasiveness and metastatic potential of lung cancer. The present study aimed to determine the potential molecular events regulating NSCLC A549 cell migration, survival and proliferation. The results indicated that: i) Mst1 was downregulated in A549 cells; ii) overexpression of Mst1 promoted A549 cell apoptosis, inhibited migration and arrested proliferation; iii) mechanistically, Mst1 activation was closely associated with mitochondrial injury, as evidenced by reduced mitochondrial potential, uncontrolled oxidative stress, pro-apoptotic protein translocation, reduced mitochondrial energy metabolism and activated caspase-9 signals; iv) at the molecular level, the ROCK1/F-actin pathway was triggered by Mst1 overexpression; and v) activated ROCK1 signaling promoted F-actin degradation and finally triggered mitochondrial apoptosis, migration impairment and proliferation delay in A549 cells. Taken together, these findings regarding A549 cell stress response lay the foundation for a detailed study into the molecular mechanism underlying cancer progression (Fig. 8). To the best of our knowledge, this is the first study to investigate the role of the Mst1-mediated ROCK1/F-actin pathway in A549 cell migration, apoptosis and proliferation, with a focus on their roles in modulating mitochondrial damage.

The association between mitochondrial homeostasis and tumor progression is an area of research that has rapidly evolved over the past decade (1). Several biological processes, including apoptosis, proliferation, metabolic reprogramming

and autophagy, are tightly linked to mitochondrial homeostasis (44), and each of these processes can be affected by alterations in mitochondrial function and structure (6). These findings have indicated that alterations in mitochondrial homeostasis may underlie many of the phenotypes that drive tumorigenic growth. In addition, mitochondrial damage has been acknowledged to have an unfavorable effect on cancer development. It has previously been reported that mitochondrial damage impairs liver cancer migration via JNK/Bcl2-interacting protein 3/sarcoendoplasmic reticulum calcium transport ATPase/Ca^{2+}/calmodulin-dependent protein kinase II pathways (8). Furthermore, alterations in mitochondrial morphology, such as mitochondrial fission, promote rectal cancer cell apoptosis (7). The mitochondrial autophagy repair system, which is also known as mitophagy, provides a survival advantage to gastric cancer (13). These data confirmed that mitochondria may be considered a potential target for regulating cancer development. In agreement with these findings, the present study demonstrated a strong association between mitochondrial injury and cancer cell migration inhibition, apoptosis and proliferation arrest. Therefore, it may be suggested that disturbance of mitochondrial integrity is of utmost importance when designing antitumor therapies in combination with chemotherapy.

The present study revealed that Mst1 affected mitochondrial injury via the ROCK1/F-actin pathway. Mst1 is a downstream factor of the Hippo pathway, which has been implicated in several pathological processes, including diabetic cardiomyopathy, osteoblast differentiation (45) and milk fat metabolism disorder (46). Furthermore, Mst1 downregulation has been identified as a potential early detection biomarker for numerous types of cancer, including colorectal cancer (47), breast cancer (48), pancreatic cancer (49), lung cancer (50) and liver cancer. At the molecular level, Mst1 has been reported to be associated with the ER stress response (51), cellular oxidative stress (52), epithelial-to-mesenchymal transition (53), transforming growth factor β-mediated tissue fibrosis (54) and mitophagy (7). The present study reported that Mst1 was downregulated in A549 cells, which was similar to previous conclusions (55). Furthermore, the present study revealed that Mst1 activation was associated with mitochondrial damage. Damaged mitochondria are particularly prone to activating the apoptotic program and mediating cellular energy disorder (11), thus leading to cancer cell death, mobilization impairment and growth arrest. This finding highlights that Mst1 dysregulation may be involved in the ability of tumor cells to escape programmed cell death. Notably, to the best of our knowledge, the present data established a novel role for Mst1 in initiating mitochondrial damage for the first time. Furthermore, it was confirmed that the ROCK1/F-actin pathway was necessary for Mst1-induced mitochondrial dysfunction and cancer cell damage. It is well documented that ROCK1 activation is strongly associated with cancer suppression. ROCK1 activation reduces the development of osteosarcoma (56), alleviates chemotherapeutic resistance in colorectal cancer (57), suppresses prostate cancer survival (16), attenuates the aggressiveness of renal cell carcinoma (17) and impairs epithelial-to mesenchymal transition in patients with lung cancer (58). Similar to these findings, the present data indicated that Mst1 overexpression-induced ROCK1 activation hampered NSCLC A549 cell migration,

proliferation and survival. These findings, combined with evidence that ROCK1 is a potentially actionable therapeutic target for tumor suppression, provided novel information regarding cancer development and may provide a novel therapeutic approach for cancer inhibition via the modulation of mitochondrial homeostasis. At present, since Mst1 lung-specific transgenic mice are currently unavailable, further *in vivo* studies using Mst1 adenoviral injection into the lung tissue of rats and/or mice to induce Mst1 overexpression are required to verify these findings.

Availability of data and materials

All data generated or analyzed during this study are included in this published article.

Authors' contributions

WQZ designed the study. JBM, KQL, JT, YXP and JZ performed the experiments. All authors participated in the discussion and revision of the manuscript.

Ethics approval and consent to participate

Not applicable.

Patient consent for publication

Not applicable.

Competing interests

The authors have declared that they have no competing interests.

References

1. Ilie M, Benzaquen J, Hofman V, Lassalle S, Yazbeck N, Leroy S, Heeke S, Bence C, Mograbi B, Glaichenhaus N, *et al*: Immunotherapy in non-small cell lung cancer: Biological principles and future opportunities. Curr Mol Med 17: 527-540, 2017.
2. Zhang Y, Lian J and Wang X: Actein inhibits cell proliferation and migration and promotes cell apoptosis in human non-small cell lung cancer cells. Oncol Lett 15: 3155-3160, 2018.
3. Patel SH, Camargo FD and Yimlamai D: Hippo signaling in the liver regulates organ size, cell fate, and carcinogenesis. Gastroenterology 152: 533-545, 2017.
4. Liu M, Liu S, Tan W, Tang F, Long J, Li Z, Liang B, Chu C and Yang J: Gaseous signalling molecule SO$_2$ via Hippo-MST pathway to improve myocardial fibrosis of diabetic rats. Mol Med Rep 16: 8953-8963, 2017.
5. Zhang M, Lin J, Wang S, Cheng Z, Hu J, Wang T, Man W, Yin T, Guo W, Gao E, *et al*: Melatonin protects against diabetic cardiomyopathy through Mst1/Sirt3 signaling. J Pineal Res: Jun 9, 2017 (Epub ahead of print). doi: 10.1111/jpi.12418.

6. Zhao Q, Ye M, Yang W, Wang M, Li M, Gu C, Zhao L, Zhang Z, Han W, Fan W, *et al*: Effect of Mst1 on endometriosis apoptosis and migration: Role of Drp1-related mitochondrial fission and Parkin-required mitophagy. Cell Physiol Biochem 45: 1172-1190, 2018.

7. Li Q, Qi F, Meng X, Zhu C and Gao Y: Mst1 regulates colorectal cancer stress response via inhibiting Bnip3-related mitophagy by activation of JNK/p53 pathway. Cell Biol Toxicol 34: 263-277, 2018.

8. Shi C, Cai Y, Li Y, Li Y, Hu N, Ma S, Hu S, Zhu P, Wang W and Zhou H: Yap promotes hepatocellular carcinoma metastasis and mobilization via governing cofilin/F-actin/lamellipodium axis by regulation of JNK/Bnip3/SERCA/CaMKII pathways. Redox Biol 14: 59-71, 2018.

9. Lee MS, Yin TC, Sung PH, Chiang JY, Sun CK and Yip HK: Melatonin enhances survival and preserves functional integrity of stem cells: A review. J Pineal Res: Jan 23, 2017 (Epub ahead of print). doi: 10.1111/jpi.12372.

10. Zhu H, Jin Q, Li Y, Ma Q, Wang J, Li D, Zhou H and Chen Y: Melatonin protected cardiac microvascular endothelial cells against oxidative stress injury via suppression of IP3R-[Ca^{2+}]c/VDAC-[Ca^{2+}]m axis by activation of MAPK/ERK signaling pathway. Cell Stress Chaperones 23: 101-113, 2018.

11. Zhou H, Wang J, Zhu P, Hu S and Ren J: Ripk3 regulates cardiac microvascular reperfusion injury: The role of IP3R-dependent calcium overload, XO-mediated oxidative stress and F-action/filopodia-based cellular migration. Cell Signal 45: 12-22, 2018.

12. Yan H, Xiao F, Zou J, Qiu C, Sun W, Gu M and Zhang L: NR4A1-induced increase in the sensitivity of a human gastric cancer line to TNFα-mediated apoptosis is associated with the inhibition of JNK/Parkin-dependent mitophagy. Int J Oncol 52: 367-378, 2018.

13. Yan H, Qiu C, Sun W, Gu M, Xiao F, Zou J and Zhang L: Yap regulates gastric cancer survival and migration via SIRT1/Mfn2/mitophagy. Oncol Rep 39: 1671-1681, 2018.

14. Li H, He F, Zhao X, Zhang Y, Chu X, Hua C, Qu Y, Duan Y and Ming L: YAP inhibits the apoptosis and migration of human rectal cancer cells via suppression of JNK-Drp1-mitochondrial fission-HtrA2/Omi pathways. Cell Physiol Biochem 44: 2073-2089, 2017.

15. Tang X, Guo D, Lin C, Shi Z, Qian R, Fu W, Liu J, Li X and Fan L: hCLOCK causes Rho-kinase-mediated endothelial dysfunction and NF-κB-mediated inflammatory responses. Oxid Med Cell Longev 2015: 671839, 2015.

16. Mu D, Zhou G, Li J, Su B and Guo H: Ursolic acid activates the apoptosis of prostate cancer via ROCK/PTEN mediated mito-chondrial translocation of cofilin-1. Oncol Lett 15: 3202-3206, 2018.

17. Zhang X, Li P, Ding Z, Wang H, Wang J, Han L and Ding S: The putative tumor suppressor, miR-199a, regulated by Snail, modulates clear cell renal cell carcinoma aggressiveness by repressing ROCK1. OncoTargets Ther 11: 103-112, 2017.

18. Zhao WH, Huang BT, Zhang JY and Zeng QC: Distinct EphB4-mediated mechanisms of apoptotic and resistance to dasatinib in human chronic myeloid leukemia and K562 cell lines. Leuk Res 63: 28-33, 2017.

19. Wang Y, Zhang Y, Yang T, Zhao W, Wang N, Li P, Zeng X and Zhang W: Long non-coding RNA MALAT1 for promoting metastasis and proliferation by acting as a ceRNA of miR-144-3p in osteosarcoma cells. Oncotarget 8: 59417-59434, 2017.

20. Vennin C, Rath N, Pajic M, Olson MF and Timpson P: Targeting ROCK activity to disrupt and prime pancreatic cancer for chemotherapy. Small GTPases: Oct 3, 2017 (Epub ahead of print). doi: 10.1080/21541248.2017.1345712.

21. Le Cras TD, Mobberley-Schuman PS, Broering M, Fei L, Trenor CC III and Adams DM: Angiopoietins as serum biomarkers for lymphatic anomalies. Angiogenesis 20: 163-173, 2017.

22. Zhang W, Tao A, Lan T, Cepinskas G, Kao R, Martin CM and Rui T: Carbon monoxide releasing molecule-3 improves myocardial function in mice with sepsis by inhibiting NLRP3 inflammasome activation in cardiac fibroblasts. Basic Res Cardiol 112: 16, 2017.

23. Zhou H, Shi C, Hu S, Zhu H, Ren J and Chen Y: BI1 is associated with microvascular protection in cardiac ischemia reperfusion injury via repressing Syk-Nox2-Drp1-mitochondrial fission pathways. Angiogenesis 21: 599-615, 2018.

24. García-Niño WR, Correa F, Rodríguez-Barrena JI, León-Contreras JC, Buelna-Chontal M, Soria-Castro E, Hernández-Pando R, Pedraza-Chaverri J and Zazueta C: Cardioprotective kinase signaling to subsarcolemmal and inter-fibrillar mitochondria is mediated by caveolar structures. Basic Res Cardiol 112: 15, 2017.

25. Ackermann M, Kim YO, Wagner WL, Schuppan D, Valenzuela CD, Mentzer SJ, Kreuz S, Stiller D, Wollin L and Konerding MA: Effects of nintedanib on the microvascular architecture in a lung fibrosis model. Angiogenesis 20: 359-372, 2017.

26. Zhou H, Yang J, Xin T, Zhang T, Hu S, Zhou S, Chen G and Chen Y: Exendin-4 enhances the migration of adipose-derived stem cells to neonatal rat ventricular cardiomyocyte-derived conditioned medium via the phosphoinositide 3-kinase/Akt-stromal cell-derived factor-1α/CXC chemokine receptor 4 pathway. Mol Med Rep 11: 4063-4072, 2015.

27. Kalyanaraman B: Teaching the basics of cancer metabolism: Developing antitumor strategies by exploiting the differences between normal and cancer cell metabolism. Redox Biol 12: 833-842, 2017.

28. Das N, Mandala A, Naaz S, Giri S, Jain M, Bandyopadhyay D, Reiter RJ and Roy SS: Melatonin protects against lipid-induced mitochondrial dysfunction in hepatocytes and inhibits stellate cell activation during hepatic fibrosis in mice. J Pineal Res: Mar 27, 2017 (Epub ahead of print). doi: 10.1111/jpi.12404.

29. Alghanem AF, Wilkinson EL, Emmett MS, Aljasir MA, Holmes K, Rothermel BA, Simms VA, Heath VL and Cross MJ: RCAN1.4 regulates VEGFR-2 internalisation, cell polarity and migration in human microvascular endothelial cells. Angiogenesis 20: 341-358, 2017.

30. Vargas LA, Velasquez FC and Alvarez BV: Compensatory role of the NBCn1 sodium/bicarbonate cotransporter on Ca^{2+}-induced mitochondrial swelling in hypertrophic hearts. Basic Res Cardiol 112: 14, 2017.

31. Jovancevic N, Dendorfer A, Matzkies M, Kovarova M, Heckmann JC, Osterloh M, Boehm M, Weber L, Nguemo F, Semmler J, *et al*: Medium-chain fatty acids modulate myocardial function via a cardiac odorant receptor. Basic Res Cardiol 112: 13, 2017.

32. Zhou H, Wang S, Hu S, Chen Y and Ren J: ER-mitochondria microdomains in cardiac ischemia-reperfusion injury: A fresh perspective. Front Physiol 9: 755, 2018.

33. Ligeza J, Marona P, Gach N, Lipert B, Miekus K, Wilk W, Jaszczynski J, Stelmach A, Loboda A, Dulak J, *et al*: MCPIP1 contributes to clear cell renal cell carcinomas development. Angiogenesis 20: 325-340, 2017.

34. Ronchi C, Torre E, Rizzetto R, Bernardi J, Rocchetti M and Zaza A: Late sodium current and intracellular ionic homeostasis in acute ischemia. Basic Res Cardiol 112: 12, 2017.

35. Couto JA, Ayturk UM, Konczyk DJ, Goss JA, Huang AY, Hann S, Reeve JL, Liang MG, Bischoff J, Warman ML, *et al*: A somatic GNA11 mutation is associated with extremity capillary malformation and overgrowth. Angiogenesis 20: 303-306, 2017.

36. Xiao L, Xu X, Zhang F, Wang M, Xu Y, Tang D, Wang J, Qin Y, Liu Y, Tang C, *et al*: The mitochondria-targeted antioxidant MitoQ ameliorated tubular injury mediated by mitophagy in diabetic kidney disease via Nrf2/PINK1. Redox Biol 11: 297-311, 2017.

37. Pickard JMJ, Burke N, Davidson SM and Yellon DM: Intrinsic cardiac ganglia and acetylcholine are important in the mechanism of ischaemic preconditioning. Basic Res Cardiol 112: 11, 2017.

38. Torres-Estay V, Carreño DV, Fuenzalida P, Watts A, San Francisco IF, Montecinos VP, Sotomayor PC, Ebos J, Smith GJ and Godoy AS: Androgens modulate male-derived endothelial cell homeostasis using androgen receptor-dependent and receptor-independent mechanisms. Angiogenesis 20: 25-38, 2017.

39. Randriamboavonjy V, Kyselova A, Elgheznawy A, Zukunft S, Wittig I and Fleming I: Calpain 1 cleaves and inactivates prosta-cyclin synthase in mesenteric arteries from diabetic mice. Basic Res Cardiol 112: 10, 2017.

40. Zhou H, Yue Y, Wang J, Ma Q and Chen Y: Melatonin therapy for diabetic cardiomyopathy: A mechanism involving Syk-mitochondrial complex I-SERCA pathway. Cell Signal 47: 88-100, 2018.

41. Li R, Xin T, Li D, Wang C, Zhu H and Zhou H: Therapeutic effect of Sirtuin 3 on ameliorating nonalcoholic fatty liver disease: The role of the ERK-CREB pathway and Bnip3-mediated mitophagy. Redox Biol 18: 229-243, 2018.

42. Tamura H, Kawamoto M, Sato S, Tamura I, Maekawa R, Taketani T, Aasada H, Takaki E, Nakai A, Reiter RJ, *et al*: Long-term melatonin treatment delays ovarian aging. J Pineal Res: Jan 23, 2017 (Epub ahead of print). doi: 10.1111/jpi.12381.

43. Zhou H, Zhu P, Wang J, Zhu H, Ren J and Chen Y: Pathogenesis of cardiac ischemia reperfusion injury is associated with CK2α-disturbed mitochondrial homeostasis via suppression of FUNDC1-related mitophagy. Cell Death Differ 25: 1080-1093, 2018.

44. Van Nostrand JL, Bowen ME, Vogel H, Barna M and Attardi LD: The p53 family members have distinct roles during mammalian embryonic development. Cell Death Differ 24: 575-579, 2017.

45. Li W, Deng Y, Feng B and Mak KK: Mst1/2 kinases modulate glucose uptake for osteoblast differentiation and bone formation. J Bone Miner Res 33: 1183-1195, 2018.

46. Chen Z, Shi H, Sun S, Luo J, Zhang W, Hou Y and Loor JJ: miR-183 regulates milk fat metabolism via MST1 in goat mammary epithelial cells. Gene 646: 12-19, 2018.

47. Yu J, Zhai X, Li X, Zhong C, Guo C, Yang F, Yuan Y and Zheng S: Identification of MST1 as a potential early detection biomarker for colorectal cancer through a proteomic approach. Sci Rep 7: 14265, 2017.

48. Ruiz-Torres SJ, Benight NM, Karns RA, Lower EE, Guan JL and Waltz SE: HGFL-mediated RON signaling supports breast cancer stem cell phenotypes via activation of non-canonical β-catenin signaling. Oncotarget 8: 58918-58933, 2017.

49. Gao ZQ, Wang JF, Chen DH, Ma XS, Yang W, Zhe T and Dang XW: Long non-coding RNA GAS5 antagonizes the chemo-resistance of pancreatic cancer cells through down-regulation of miR-181c-5p. Biomed Pharmacother 97: 809-817, 2018.

50. Zheng X, Dong Q, Zhang X, Han Q, Han X, Han Y, Wu J, Rong X and Wang E: The coiled-coil domain of oncogene RASSF 7 inhibits hippo signaling and promotes non-small cell lung cancer. Oncotarget 8: 78734-78748, 2017.

51. Ashokkumar R, Jamuna S, Sakeena Sadullah MS and Niranjali Devaraj S: Vitexin protects isoproterenol induced post myocardial injury by modulating hipposignaling and ER stress responses. Biochem Biophys Res Commun 496: 731-737, 2018.

52. Yu L, Liu Y, Jin Y, Cao X, Chen J, Jin J, Gu Y, Bao X, Ren Z, Xu Y, *et al*: Lentivirus-mediated HDAC3 inhibition attenuates oxidative stress in APPswe/PS1dE9 mice. J Alzheimers Dis 61: 1411-1424, 2018.

53. Li X, Zhao X, Song W, Tian Z, Yang L, Niu Q, Zhang Q, Xie M, Zhou B, Xu Y, *et al*: Pseudolaric acid B inhibits proliferation, invasion and epithelial-to-mesenchymal transition in human pancreatic cancer cell. Yonsei Med J 59: 20-27, 2018.

54. Wang S, Fan Y, Feng X, Sun C, Shi Z, Li T, Lv J, Yang Z, Zhao Z and Sun D: Nicorandil alleviates myocardial injury and post-infarction cardiac remodeling by inhibiting Mst1. Biochem Biophys Res Commun 495: 292-299, 2018.

55. Zhou H, Wang J, Zhu P, Zhu H, Toan S, Hu S, Ren J and Chen Y: NR4A1 aggravates the cardiac microvascular ischemia reperfusion injury through suppressing FUNDC1-mediated mitophagy and promoting Mff-required mitochondrial fission by CK2α. Basic Res Cardiol 113: 23, 2018.

56. Su S and Nie X: miR-139 prompts the development of osteo-sarcomas mainly through targeting ROCK1. Pharmazie 72: 759-763, 2017.

57. Wang X, Sun D, Tai J, Chen S, Yu M, Ren D and Wang L: TFAP2C promotes stemness and chemotherapeutic resistance in colorectal cancer via inactivating hippo signaling pathway. J Exp Clin Cancer Res 37: 27, 2018.

58. Lin L, Li M, Lin L, Xu X, Jiang G and Wu L: FPPS mediates TGF-β1-induced non-small cell lung cancer cell invasion and the EMT process via the RhoA/Rock1 pathway. Biochem Biophys Res Commun 496: 536-541, 2018.